ORIGINAL ARTICLE



Neutrino emissivity in the color superconducting quark-hadron-mixed phase

A. Freeman¹ | D. Farrell¹ | F. Weber^{1,2,*} | W. M. Spinella³ | M. G. Orsaria^{4,5} | G. A. Contrera^{4,6}

¹Department of Physics, San Diego State University, San Diego, California ²Center for Astrophysics and Space Sciences, University of California at San Diego, La Jolla, California

³Department of Sciences, Wentworth Institute of Technology, Boston, Massachusetts

⁴Facultad de Ciencias Astronómicas y Geofísicas, UNLP, Buenos Aires, Argentina

⁵CONICET, CABA, Argentina

⁶Institute of Physics of La Plata University, CONICET, La Plata, Argentina

*Correspondence

F. Weber, Department of Physics, San Diego State University, 5500 Campanile Drive, San Diego, CA 92182-1233. Email: fweber@sdsu.edu

Funding Information

CONICET, PIP-0714. UNLP, X824, G157, G140. National Science Foundation (USA), PHY-1714068, PHY-1411708. The tremendously high pressures that exist in the cores of neutron stars may break up neutrons, protons plus other hadronic particles into their quark constituents. This transition from hadronic matter to quark matter could lead to an extended quark-hadron-mixed phase region in the cores of neutron stars that would segregate phases by net charge to minimize the total energy of the phase, leading to the formation of a crystalline quark-hadron Coulomb lattice. The neutrino emissivity due to the elastic scattering of electrons off the lattice was previously studied where it was assumed that the quark lattice sites are made of ordinary (i.e., nonsuperconducting) quark structures (blobs, rods, and slabs). In the present study, we extend these calculations to the elastic scattering of electrons off quark blobs that are in the color superconducting color-flavor-locked (CFL) phase. As this phase reduces the electric charge carried by quark blobs, the electric charge density of CFL blobs is smaller than that of non-CFL blobs. The neutrino emission rates, however, change only minimally.

KEYWORDS

color superconductivity - hadronic matter - neutron stars - quark matter

1 | INTRODUCTION

Due to the property of asymptotic freedom, it is possible that the quarks that are confined in baryons in the dense neutron star core may be freed, resulting in a first order phase transition from hadronic matter to deconfined quark matter. If the surface tension between the hadronic matter phase and the deconfined quark matter phase is sufficiently low, and charge neutrality between the two phases is treated globally as proposed by Glendenning (1992), then a mixed phase will form in which both phases of matter coexist. To minimize the Coulomb, surface, and isospin asymmetry energies, this quark-hadron-mixed phase may rearrange itself into different geometric configurations that result in positively charged regions of hadronic matter segregated from negatively charged regions of quark matter, with the rare phase geometry occupying sites on a crystalline Coulomb lattice. The presence of a quark-hadron Coulomb lattice will cause an increase in the neutrino emissivity from the neutron star core, with neutrino-antineutrino pairs being created by electrons that are scattered from quark-hadron lattice structures via the Coulomb interaction, a process we refer to as mixed-phase bremsstrahlung (MPB). This process is similar to that of neutrino-pair bremsstrahlung in the neutron star crust, where electrons scatter from an ion lattice, and for which a large body of work already exists (see Kaminker et al. 1999 and references therein). The neutrino emissivity due to MPB was previously calculated for different mixed phase geometries in Na et al. (2012), Spinella et al. (2016), Spinella (2017), and Spinella et al. (2018), with the assumption that the quark lattice sites are nonsuperconducting. In this work, we extend these calculations to include quark structures that are in a color-flavor-locked (CFL) superconducting phase, and compare these to previous calculations of MPB neutrino emissivity and to that of other possible neutrino-generating mechanisms in the neutron star core.

2 | HADRONIC MATTER

The nonlinear relativistic mean-field approximation is used to model the hadronic matter inside of neutron stars. The Lagrangian of this model is given by (Spinella et al. 2016)

$$\mathcal{L} = \sum_{\mathbf{B}} \overline{\psi}_{\mathbf{B}} \left[\gamma_{\mu} \left(i \partial^{\mu} - g_{\omega \mathbf{B}} \omega^{\mu} - \frac{1}{2} g_{\rho \mathbf{B}} \tau \cdot \rho^{\mu} \right) - (m_{n} - g_{\sigma \mathbf{B}} \sigma) \right] \psi_{\mathbf{B}}$$

$$+ \frac{1}{2} (\partial_{\mu} \sigma \partial^{\mu} \sigma - m_{\sigma}^{2} \sigma^{2}) - \frac{1}{4} \omega_{\mu \nu} \omega^{\mu \nu} + \frac{1}{2} m_{\omega}^{2} \omega_{\mu} \omega^{m u}$$

$$+ \frac{1}{2} m_{\rho}^{2} \rho_{\mu} \rho^{\mu} - \frac{1}{4} \rho_{\mu \nu} \rho^{\mu \nu} + \frac{1}{3} b_{\sigma} m_{N} (g_{\sigma N} \sigma)^{3}$$

$$+ \frac{1}{4} c_{\sigma} m_{N} (g_{\sigma N} \sigma)^{4} + \sum_{\lambda = \sigma} \overline{\psi}_{\lambda} (i \gamma_{\mu} \partial^{\mu} - m_{\lambda}) \psi_{\lambda}. \tag{1}$$

where $\psi_{\rm B}$ denotes baryon fields $(B=n,\ p,\ \Sigma,\ \Lambda,\ \Xi),\ \psi_{\lambda}$ denotes electrons and muons, and the field tensors $\omega_{\mu\nu}$ and $\rho_{\mu\nu}$ are defined as $\omega_{\mu\nu}=\partial_{\mu}\omega_{\nu}-\partial_{\nu}\omega_{\mu}$ and $\rho_{\mu\nu}=\partial_{\mu}\rho_{\nu}-\partial_{\nu}\rho_{\mu}$. The values of the coupling constants and meson masses are $g_{\sigma N}=9.7744,\ g_{\omega N}=10.746,\ g_{\rho N}=7.8764,\ b_{\sigma}=0.003798,\ c_{\sigma}=-0.003197,\ m_{\sigma}=550$ MeV, $m_{\omega}=783$ MeV, and $m_{\rho}=763$ MeV (the SWL (Spinella-Weber model L) of Spinella et al. (2016)). The conditions of electric charge neutrality and chemical equilibrium of neutron star matter lead to

$$0 = \sum_{R} n_{B} q_{B} + \sum_{\lambda} n_{\lambda} q_{\lambda}, \qquad (2)$$

$$\mu_i = b_i \mu_N - q_i \mu_e, \tag{3}$$

with μ_i , b_i , and q_i denoting the chemical potential, baryon number, and electrical charge of particle i. The quantities $n_{\rm B}$ and n_{λ} in Equation (2) are the number densities of baryons and leptons, respectively. Equations (2) and (3) need to be solved for the meson mean fields σ , ω_0 , and ρ_{03} alongside the equations of motion that follow from Equation (1). The equation of state, $p(\varepsilon)$ of the hadronic system is then obtained from (Spinella 2017; Spinella et al. 2016)

$$\varepsilon_{\rm H} = \frac{1}{3} b_{\sigma} m_N (g_{\sigma} \sigma)^3 + \frac{1}{4} c_{\sigma} (g_{\sigma} \sigma)^4 + \frac{1}{2} m_{\sigma}^2 \sigma^2
+ \frac{1}{2} m_{\omega}^2 \omega_0^2 + \frac{1}{2} m_{\rho}^2 \rho_{03}^2
+ \sum_{\rm B} \frac{2J_{\rm B} + 1}{2\pi^2} \int_0^{k_B} \sqrt{k^2 + m_B^{*2}} k^2 dk + \varepsilon_L$$
(4)

and

$$p_{\rm H} = -\frac{1}{3}bm_n(g_\sigma\sigma)^3 - \frac{1}{4}c(g_\sigma\sigma)^4 - \frac{1}{2}m_\sigma^2\sigma^2 + \frac{1}{2}m_\omega^2\omega_0^2 + \frac{1}{2}m_\rho^2\rho_{03}^2 + \frac{1}{3}\sum_B \frac{2J_{\rm B} + 1}{2\pi^2} \int_0^{k_B} \frac{k^4dk}{\sqrt{k^2 + m_{\rm B}^{*2}}} + p_{\rm L}.$$
 (5)

here, $m_{\rm B}^* = m_{\rm B} - g_{\sigma \rm B} \sigma$ is the effective baryon mass in matter, and $k_{\rm B}$ and k_{λ} are the Fermi momenta of baryons and leptons, respectively. The quantities $\varepsilon_{\rm L}$ and $p_{\rm L}$ in Equations (4) and (5) denote the energy density and pressure of the leptons (Spinella 2017, Spinella et al. 2016).

3 | QUARK MATTER

The nonlocal 3-flavor Nambu-Jona-Lasinio model is used to describe the quark matter phase. The thermodynamic potential of the deconfined quark phase is given by (Orsaria et al. 2013, 2014; Spinella et al. (2016))

$$\Omega = -\frac{3}{\pi^2} \sum_{f=u,d,s} \int_0^\infty dp \ln \left[\widehat{\omega_f^2} + M_f^2(\omega_f^2) \right] \frac{1}{\omega_f^2 + m_f^2} \\
-\frac{3}{\pi^2} \sum_{f=u,d,s} \int_0^{\sqrt{\mu_f^2 - m_f^2}} dp p^2 [(\mu_f - E_f)\theta(\mu_f - m_f)] \\
-\frac{1}{2} \left[\sum_{f=u,d,s} \left(\overline{\sigma_f} \overline{S}_f + \frac{G_S}{2} \overline{S}_f^2 \right) + \frac{H}{2} \overline{S}_u \overline{S}_d \overline{S}_s \right] \\
-\sum_{f=u,d,s} \frac{\overline{\omega_f^2}}{4G_V}.$$
(6)

Equation (6) contains the scalar and vector quark mean fields $\overline{\sigma}_f$ and $\overline{\omega}_f$, respectively, while \overline{S}_f is an auxiliary mean field associated with quark flavor f. The pressure and energy density of the quark phase are obtained from Equation (6) as follows (Orsaria et al. 2013, 2014; Spinella et al. 2016):

$$p_{\mathcal{O}} = \Omega(\mu_f = \overline{\omega_f} = 0) - \Omega_0, \tag{7}$$

$$\varepsilon_{\mathbf{Q}} = -p_{\mathbf{Q}} + \sum_{f=u,d,s} \rho_f \mu_f + \sum_{\lambda=e^-,\mu^-} \rho_{\lambda} \mu_{\lambda}, \tag{8}$$

where Ω_0 is fixed by the condition that $\Omega = 0$ at zero quark densities.

4 | QUARK-HADRON-MIXED PHASE

Using the hadronic model of Section 2 and the quark model of Section 3, the Gibbs condition

$$p_{\rm H}(\mu_n, \ \mu_e, \ T=0) = p_{\rm O}(\mu_n, \ \mu_e, \ T=0)$$
 (9)

is used to determine the pressure and energy density in the quark-hadron-mixed phase (Glendenning 1992, 2001; Spinella et al. 2016). The pressure in the mixed phase $p_{\rm M}$ is expressed as

$$p_{\rm M} = \frac{1}{2}(p_{\rm H} + p_{\rm Q}),\tag{10}$$

and the energy density $\varepsilon_{\rm M}$ is given by

$$\varepsilon_{\rm M} = (1 - \chi)\varepsilon_{\rm H} + \chi\varepsilon_{\rm O},$$
 (11)

where the quantity χ is the fraction of quark matter to total matter in the mixed phase.

The matter inside of the mixed phase will arrange itself so that the total energy is minimized. To minimize the energy, the rare phase will assume certain lattice structures. The lattice configurations are assumed to be spherical blobs, rods, and slabs. As the density increases in the mixed phase, the rare phase changes its lattice configuration from blobs to rods to slabs. For $\chi \leq .5$, deconfined quarks are the rare phase, and hadrons are the rare phase when $.5 \leq \chi \leq 1.0$. Once $\chi \geq .5$, the hadronic matter evolves from slabs to rods to blobs

(Glendenning 1992, 2001). For the SWL hybrid equation of state used in this article, one finds $\chi \leq .39$ corresponding to a quark-hadron lattice made up of spherical blobs, rods, and slabs of quark matter with a gravitational mass close to $.1M_{\odot}$. However, for the purposes of this work, we will consider only the spherical blob geometry. The size of the quark-hadron lattice depends on the stellar central density and, therefore, on the star's rotational frequency. Numerical studies have shown that the quark-hadron lattice vanishes if the star performs more than around 350 rotations per second.

4.1 | CFL quark blobs

For this study, we assume that the quark blobs are made up of either ordinary non-color superconducting color-flavor locked (nCFL) quark matter or color superconducting quark matter in the CFL phase. The crucial difference between nCFL and CFL quark matter concerns the equality of all quark Fermi momenta in CFL quark matter, which leads to charge neutrality in bulk without any need for electrons (Rajagopal & Wilczek 2001). This has important consequences for the charge-to-mass ratios of quark blobs. For nCFL quark blobs, the charge is approximately

$$Z \approx .1 \ m_{150}^2 \ A, \qquad A \ll 10^3,$$
 (12)

$$Z \approx 8 \ m_{150}^2 \ A^{1/3}, \qquad A \gg 10^3,$$
 (13)

where $m_{150} \equiv m_s/150$ and $m_s = 119 \, \mathrm{MeV}$ is the mass of the strange quark. For small A, the charge is the volume quark charge density multiplied by the quark blob volume with a result that is proportional to A itself. This relation holds until the system grows larger than around 5 fm, or $A \approx 150$, at which point the charge is mainly distributed near the quark blob surface, and $Z \propto A^{1/3}$ (Madsen 2001). In contrast to this, the charge-to-mass ratio of CFL quark blobs is described by Madsen (2001).

$$Z \approx .3 \ m_{150} \ A^{2/3}$$
. (14)

We use these relations to study the consequences of CFL color superconductivity for a quark-hadron lattice in the cores of neutron stars.

4.2 | Surface tension

The surface tension of the quark-hadron-mixed phase can be expressed as (Glendenning 1992, 2001)

$$\alpha(\chi) = \eta L[\varepsilon_{Q}(\chi) - \varepsilon_{H}(\chi)], \tag{15}$$

where $\varepsilon_{\rm Q}$ and $\varepsilon_{\rm H}$ are the total energy densities of the quark and hadronic phase, respectively. The quantity L is around 1 fm, and η is a proportionality constant that is used to ensure that the surface tension remains less than 70 MeV fm⁻² (see Spinella et al. 2016, 2018, and references therein).

5 | THE RARE PHASE

To calculate the radius of the rare phase geometries r, the sum of the Coulomb and surface energies must be minimized, and

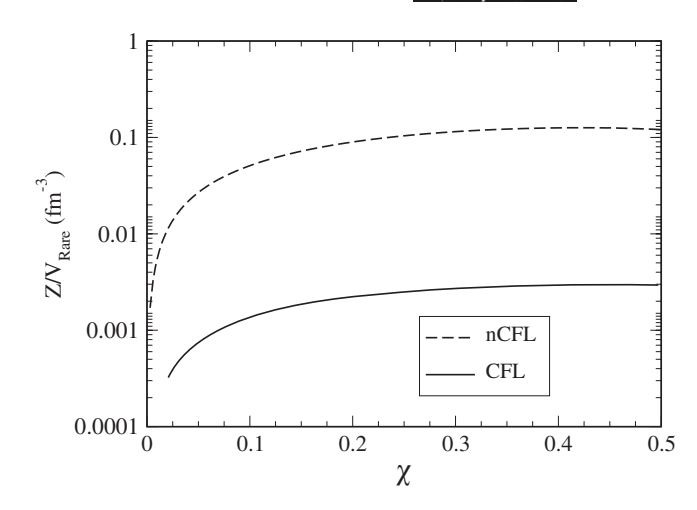


FIGURE 1 Charge number per unit volume of quark blobs, made of either nCFL or color-flavor-locked (CFL) quark matter, as a function of the quark fraction in the mixed phase, γ

then solved for r. The charge density of the mixed phase is set to be uniform throughout the phase. The charge number Z per unit volume $V_{\rm Rare}$ is plotted as a function of χ in Figure 1. Because of the reduced electric charge carried by CFL quark blobs (see Equations (12)–(14)), the charge density $Z/V_{\rm Rare}$ is smaller if quark blobs are in the CFL phase.

6 | NEUTRINO EMISSIVITIES

In this section, we investigate the effect that a crystalline quark-hadron-mixed phase would have on the emission of neutrinos from the cores of neutron stars. These neutrinos would be produced through elastic electron-quark blob scattering, henceforth referred to as quark bremstrahlung. A very similar process occurs in the crusts of neutron stars, where the rare phase structures are made up of heavy ionized atomic nuclei (Flowers 1973, Itoh et al. 1984, Itoh et al. 1984a, Itoh et al. 1984b, Itoh et al. 1984c, Pethick et al. 1997, Kaminker et al. 1999), as opposed to quarks or hadrons studied in our case. However, both types of structures are surrounded by a free relativistic electron gas, resulting in the scattering of electrons and the creation of neutrino-antineutriono pairs. The other standard processes that contribute to the production of neutrinos are neutrino pair bremsstrahlung (NPB), the direct Urca process (DU), and the modified Urca (MU) process.

6.1 | Elastic neutrino-pair bremsstrahlung

Elastic neutrino-pair bremsstrahlung creates neutrinos through the reaction $B_1 + B_2 \rightarrow B_1 + B_2 + v + \overline{v}$, where B_1 and B_2 denoted baryons of type B. The neutrino emissivities for this reaction have been calculated for (n, n), (n, p), and for (p, p). Because the NPB process is less efficient for heavier baryons (Yakovlev et al. 2001), only (n, n), (n, p), and for (p, p) processes are considered in our study. The neutrino

emissivity for NPB between two neutrons is given by

$$\varepsilon_{\text{NPB}}^{(nn)} = 7.434 \times 10^{19} \left(\frac{m_n^*}{m_n}\right)^4 \left(\frac{n_n}{n_0}\right)^{\frac{1}{3}} T_9^8 \text{ ergs s}^{-1} \text{ cm}^{-3},$$
(16)

where $T_9 \equiv T/(10^9 \text{ K})$. The neutrino emissivity for NPB between a proton and a neutron is given by

$$\varepsilon_{\text{NPB}}^{(np)} = 3.1482 \times 10^{20} \left(\frac{m_n^* m_p^*}{m_n m_p} \right)^2 \left(\frac{n_p}{n_0} \right)^{\frac{1}{3}} T_9^8 \text{ ergs s}^{-1} \text{ cm}^{-3},$$
(17)

and the emissivity for NPB between two protons has the form

$$\varepsilon_{\text{NPB}}^{(pp)} = 1.7325 \times 10^{19} \left(\frac{m_p^*}{m_p}\right)^4 \left(\frac{n_p}{n_0}\right)^{\frac{1}{3}} T_9^8 \text{ ergs s}^{-1} \text{ cm}^{-3}.$$
(18)

The neutrino emissivity for the quark analog of the NPB process was derived by Iwamoto (1982). It is given by

$$\varepsilon_{\text{NPB}}^{(qq)} = 2.98 \times 10^{19} \frac{1}{n_0} \sum_{f} n_f T_9^8 \text{ ergs s}^{-1} \text{ cm}^{-3}.$$
 (19)

6.2 | DU process

The DU process $B_1 \rightarrow B_2 + e^- + \overline{\nu}$ and its back-reaction $B_2 + e^- \rightarrow B_1 + \nu$ give the largest contribution to the total neutrino emissivity. The neutrino emissivity for the DU process is expressed as (Lattimer et al. 1991)

$$\varepsilon_{\rm DU}^{(B_1 B_2)} = 4.00 \times 10^{27} \left(\frac{n_e}{n_0}\right)^{\frac{1}{3}} \frac{m_{B_1} m_{B_2}}{m_n^2} R T_9^6 \text{ erg s}^{-1} \text{ cm}^{-3},$$
(20)

where R = 1. The DU process for quarks is represented by the reactions $d \to u + e^- + \overline{v}$ and $u + e^- \to d + v$. The corresponding neutrino emissivities for the quark DU process have the form (Iwamoto 1982)

$$\varepsilon_{\text{DU}}^{(qq)} = 8.8 \times 10^{26} \alpha_s \frac{1}{n_0} \sum_f n_f T_9^8 \text{ erg s}^{-1} \text{ cm}^{-3},$$
 (21)

where $\alpha_s = .1181$ denotes the strong coupling constant.

6.3 | MU process

The MU process, where the presence of an additional by stander particle (B_3) is required to conserve energy and momentum, is represented by the following reactions (Yakovlev et al. 2001): $B_1 + B_3 \rightarrow B_2 + B_3 + e^- + \overline{\nu}$ and $B_2 + B_3 + e^- \rightarrow B_1 + B_3 + \nu$. These reactions give the following neutrino emission rates for neutrons and protons, respectively:

$$\varepsilon_{\text{MU}}^{(n)} = 5.814 \times 10^{19} \left(\frac{m_n^*}{m_n}\right)^3 \left(\frac{m_p^*}{m_p}\right) \left(\frac{n_e}{n_0}\right)^{\frac{1}{3}} T_9^8 \kappa$$

$$\times \text{ erg s}^{-1} \text{ cm}^{-3} \tag{22}$$

$$\varepsilon_{\text{MU}}^{(p)} = 5.8004 \times 10^{19} \left(\frac{m_p^*}{m_p}\right)^3 \left(\text{most sign}^{-1} \text{ cm}^{-3},\right)$$

$$\varepsilon_{\text{MU}}^{(p)} = 5.8004 \times 10^{19} \left(\frac{m_p^*}{m_p}\right)^3 \left(\frac{m_n^*}{m_n}\right) \left(\frac{n_e}{n_0}\right)^{\frac{1}{3}} T_9^8 F_p \kappa$$

$$\times \text{ erg s}^{-1} \text{ cm}^{-3}, \tag{23}$$

where $\kappa = 1.76 - .63(n_n/n_0)^{-\frac{2}{3}}$ and F_n is given by

$$F_p = \left(n_e^{\frac{1}{3}} + 3n_p^{\frac{1}{3}} - n_n^{\frac{1}{3}}\right)^2 \left(8n_e^{\frac{1}{3}}n_p^{\frac{1}{3}}\right)^{-1}.$$
 (24)

The MU process for quarks is given by the reactions d + $q_1 \rightarrow u + q_1 + e^- + \overline{v}$ and $u + q_1 + e^- \rightarrow d + q_1 + v$. The neutrino emissivities for the quark MU process are given by

$$\varepsilon_{\text{MU}}^{(qq)} = 2.83 \times 10^{19} \alpha_{\text{s}}^2 \frac{1}{n_0} \sum_{f} n_f T_9^8 \text{ ergs s}^{-1} \text{ cm}^{-3}.$$
 (25)

6.4 The quark-hadron-mixed-phase contribution

Modeling the interactions of electrons with a background of neutrons, protons, hyperons, muons, and quarks is an exceptionally complicated problem. However, to determine the neutrino emissivity that is due to elastic electron-lattice interactions in the quark-hadron-mixed phase, we need to consider only the Coulomb interaction between them. This simplifies the problem greatly, as a significant body of work exists for the analogous process of electron-ion scattering that takes place in the crusts of neutron stars (see references in Kaminker et al. 1999, Spinella et al. 2016, 2018).

To determine the state of the lattice in quark-hadron-mixed phase, we use the dimensionless ion coupling parameter given by $\Gamma = Z^2 e^2 / (Rk_B T)$, where R denotes the ideal gas constant and k_B the Boltzmann constant (Haensel et al. 2007). Below $\Gamma_{melt} = 175$, the lattice behaves as a Coulomb liquid, and above as a Coulomb crystal (Haensel et al. 2007). It was shown by Na et al. (2012) that the emissivity due to electron-blob interactions in the mixed phase was insignificant compared to other contributions at temperatures above $T \gtrsim 10^{10}$ K. Therefore, in this work we consider temperatures in the range $10^7 \text{ K} \le T \le 10^{10}$ K. At these temperatures, the value of the ion coupling parameter is generally above Γ_{melt} , and so the lattice in the quark-hadron-mixed phase is taken to be a Coulomb crystal.

To account for the fact that the elasticity of scattering events is temperature dependent, we need to compute the Debye-Waller factor, W(q), which depends on the plasma temperature $T_p = \hbar \omega_p / k_B$ and on the plasma frequency $\omega_p =$ $\sqrt{4\pi Z^2 e^2 n_b/m_b}$. The value of the Debye–Waller factor for spherical blobs, which are studied in this article, is given by

$$W(q) = \frac{\alpha q^2}{8k_e^2} (1.399e^{-9.1t_p} + 12.972t_p), \tag{26}$$

where q is the phonon scattering wave vector, the quantity $\alpha = 4\hbar^2 k_e^2/(k_B T_p m_b)$, and $t_p = T/T_p$, with m_b the mass of the spherical blob (Kaminker et al. 1999). Once the Debye-Waller factor was calculated, the effective electron-lattice interaction can be calculated (for details, see

143

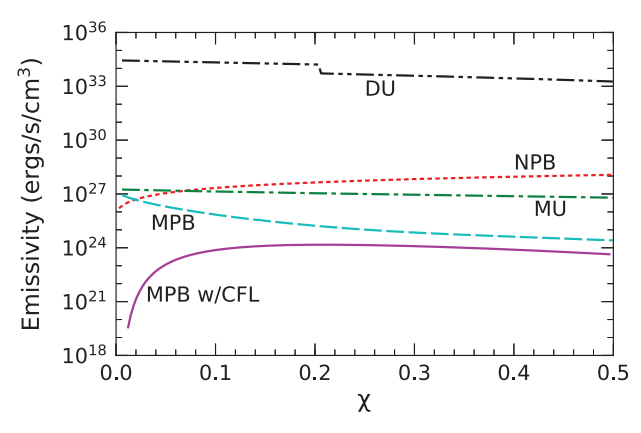


FIGURE 2 Neutrino emissivity as a function of χ for matter at a temperature of $T=10^{10}$ K. The neutrino emissivity has contributions from the direct Urca (DU) process, modified Urca (MU) process, nucleon-nucleon quark-quark neutrino pair bremsstrahlung (NPB), and mixed phase bremsstrahlung (MPB)

Spinella 2017, and Spinella et al. 2016, 2018). The general expression for the emission of neutrinos due to MPB was derived by Haensel et al. (1996). For blobs, one has

$$\varepsilon_{\text{MPR}}^{\text{blobs}} = 5.37 \times 10^{20} n T_0^6 Z^2 L \text{ erg s}^{-1} \text{ cm}^{-3},$$
 (27)

where n is the number density of rare phase spherical blobs. The quantity $L(\equiv L_{\rm sl} + L_{\rm ph})$ is dimensionless and takes into account the neutrino emissivities from Bragg-scattering, $L_{\rm sl}$, and from phonons, $L_{\rm ph}$. For this study, only the neutrino emissivities from the Bragg scattering contribute. The contribution from the phonons is insignificant compared to that of the Bragg-scattering, so $L_{\rm ph} = 0$.

7 | RESULTS

Figures 2 and 3 show the neutrino emissivities for temperatures of 10¹⁰ and 10⁷ K, respectively. For both cases, the DU process dominates at all temperatures. As the temperature decreases, the neutrino emissivities for the DU process drop drastically, but still dominate over the other processes. The neutrino emissivities due to the MU and NPB processes are also heavily effected by the temperature of the star. As temperature decreases, the neutrino emissivities from these processes become smaller.

The neutrino emissivity contribution from the MPB is the only process that is effected by the implementation of color superconductivity. Let us first analyze the neutrino emissivity from MPB for nFCL quark matter. This process peaks at very low χ values. The neutrino emissivities should be at their highest for this process when the rare phase assumes the geometry of spherical blobs, which occurs at low χ values. One sees that there is a steady decrease in the neutrino emissivity for this process as χ increases, which is due to the fact that $L_{\rm sl}$ is dependent on the sum of scattering wave vectors $|\mathbf{K}| \leq 2k_{\rm e}$, where $k_{\rm e}$ is the electron Fermi momentum. The number of scattering vectors that satisfy $|\mathbf{K}| \leq 2k_{\rm e}$ is noted as N_K . Both $k_{\rm e}$ and N_K are at their maximums right

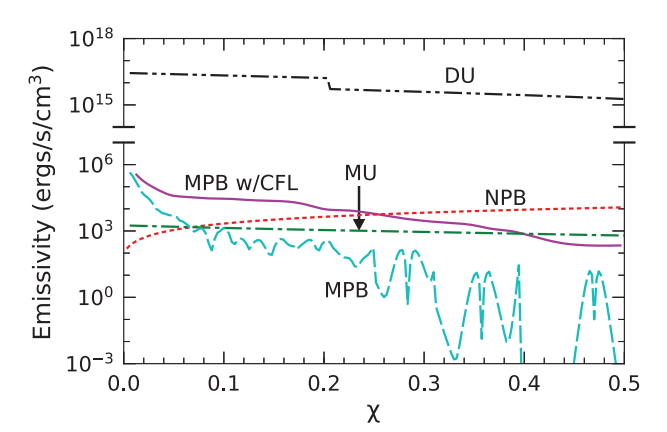


FIGURE 3 The same as Figure 2, but for a temperature of 10⁷ K

before the commencement of the mixed phase. However, as density increases within the mixed phase, the electron number density and the Fermi momentum begin to decrease. Because there are less electrons to scatter off of the lattice, the resultant number of scattering vectors N_K decreases as well. Consequently, the number of neutrinos that are produced likewise decreases. The neutrino emissivity due to the MBP process for nCFL quark matter drops drastically with temperature compared to that of other processes. This is due to the fact that the MPB process is $\propto T^6$, as opposed to the other processes that are $\propto T^8$. As discussed above, the phonon contribution to the neutrino emissivity is negligible, so all of the neutrinos that are produced in this process come from the static-lattice contribution. The MPB process is significant compared to the MU and NPB processes at temperature $T < 10^9$ K. For the MPB process for CFL quark matter, the neutrino emissivities are much smaller than that of the MPB process for nCFL quark matter. This is due to the dependence of the static-lattice contribution (L_{sl}) on the spherical blob charge $Q_{\rm Blob}$. For nCFL quark matter, $L_{\rm sl} \propto Q_{\rm Blob}^2$, which means that $L_{\rm sl} \propto (n_q V_{\rm Rare})^2$. For CFL quark matter, $L_{\rm sl}$ has the same dependence on Q_{Blob} . However, $Q_{\text{Blob}} \propto (n_q V_{\text{Rare}})^{2/3}$ for CFL quark matter, so $L_{\rm sl} \propto (n_q V_{\rm Rare})^{4/3}$. As a result, the neutrino emissivities will grow at a slower rate compared to the neutrino emissivities for nCFL quark matter.

The neutrino emissivity for the MPB process for CFL quark matter starts to decrease for the same reasons as the nCFL quark matter. The electron number density starts to decrease, which in turn forces the number of scattering vectors to decrease, resulting in the production of fewer neutrinos. The dependence of the neutrino emissivity on temperature causes the emissivities to drop drastically with a decrease in temperature. This is also due to the fact that the MPB process depends on T^6 , not T^8 like the other processes. Compared to that of other neutrino emission processes, the MPB process is less significant at higher temperatures. However, for temperatures in the range of 10^7 to 10^9 K, the MPB process is more significant compared to the NPB process. The MPB process is also more significant compared to the MU process, but only at temperatures $\leq 10^8$ K.

8 | SUMMARY

In this article, it was shown that the neutrino emissivities overall do not change much for the DU, MU, and NPB processes when the quark blobs are treated as CFL color superconductors. The neutrino emissivities due to the MPB process for CFL quark matter are lower than those for nCFL matter. This is due to the fact that the charge of the spherical blobs for CFL quark matter is less than the spherical blob charge for nCFL quark matter. It was also shown that when $T \le 10^8$ K, the MPB process for CFL quark matter is significant compared to the MU process. The MPB process is also larger than the NPB process when $T \le 10^9$ K. The DU process dominates the MPB processes and all other processes for nCFL and CFL quark matter. Hence, the MPB will only be of importance for the thermal evolution of neutron stars if the DU process is not operating. Only then the presence of a quark-hadron core in the center of a neutron star may marginally change the star's thermal evolution.

ACKNOWLEDGMENTS

This work was supported by the National Science Foundation (USA), grant numbers PHY-1411708 and PHY-1714068; Grants G140, G157, and X824 from UNLP, PIP-0714, from CONICET.

REFERENCES

Flowers, E. 1973, *ApJ*, *180*, 911. Glendenning, N. K. 1992, *Phys. Rev. D*, *46*, 1274. Glendenning, N. K. 2001, *Phys. Rep.*, *342*, 393. Haensel, P., Kaminker, A. D., & Yakovley, D. G. 1996, *A&A*, *314*, 328. Haensel, P., Potekhin, A. Y., & Yakovlev, D. G. 2007, Neutron Stars 1: Equation of State and Structure, Springer (New York).

Itoh, N., & Kohyama, Y. 1984, ApJ, 275, 858.

Itoh, N., Kohyama, Y., Matsumoto, N., & Seki, M. 1984a, ApJ, 280, 787.

Itoh, N., Kohyama, Y., Matsumoto, N., & Seki, M. 1984b, ApJ, 285, 304.

Itoh, N., Matsumoto, N., Seki, M., & Kohyama, Y. 1984c, ApJ, 279, 413.

Iwamoto, N. 1982, Ann. Phys., 141, 1.

Kaminker, A. D., Pethick, C. J., Potekhin, A. Y., Thorsson, V., & Yakovlev, D. G. 1999, A&A, 343, 1009.

Lattimer, J. M., Pethick, C. J., Prakash, M., & Haensel, P. 1991, Phys. Rev. Lett., 66, 2701.

Madsen, J. 2001, Phys. Rev. Lett., 87, 172003.

Na, X., Xu, R., Weber, F., & Negreiros, R. 2012, Phys. Rev. C, 86, 123016.

Orsaria, M., Rodrigues, H., Weber, F., & Contrera, G. A. 2013, Phys. Rev. D, 87, 023001

Orsaria, M., Rodrigues, H., Weber, F., & Contrera, G. A. 2014, Phys. Rev. C, 89, 015806.

Pethick, C. J., & Thorsson, V. 1997, Phys. Rev. D, 56, 7548.

Rajagopal, K., & Wilczek, F. 2001, Phys. Rev. Lett., 86, 3492.

Spinella, W. M. 2017, A systematic investigation of exotic matter in neutron stars, Ph.D. thesis, Claremont Graduate University, Claremont, CA and San Diego State University, San Diego, CA.

Spinella, W. M., Weber, F., Contrera, G. A., & Orsaria, M. G. 2016, Eur. Phys. J. A. 52, 61.

Spinella, W. M., Weber, F., Orsaria, M. G., & Contrera, G. A. 2018, *Universe*, 4,

Yakovlev, D. G., Kaminiker, A. D., Gnedin, O. Y., & Haensel, P. 2001, Phys. Rep., 354, 1.

How to cite this article: Freeman A, Farrell D, Weber F, Spinella WM, Orsaria MG, Contrera GA. Neutrino emissivity in the color superconducting quark-hadron-mixed phase. *Astron. Nachr.* 2019;340:139–144. https://doi.org/10.1002/asna.201913578